Research Square

Preprints are preliminary reports that have not undergone peer review.
They should not be considered conclusive, used to inform clinical practice,
or referenced by the media as validated information.

Periodic theta and spectral–memory relationships differentiate amnestic mild cognitive impairment from healthy aging

Camille Bouhour
University of Geneva
Vincent Rochas
M/EEG & Neuromod Platform
Mohamed Eshmawey
University Hospital of Geneva
Paul G. Unschuld
University of Geneva
Lucie Bréchet
lucie.brechet@unige.ch
University of Geneva

Research Article

Keywords: Amnestic mild cognitive impairment, resting-state EEG, source localization, theta oscillations, aperiodic slope, memory networks

Posted Date: November 10th, 2026

DOI: https://doi.org/10.21203/rs.3.rs-11277287/v1

License: This work is licensed under a Creative Commons Attribution 4.0 International License.
Read Full License

Additional Declarations: No competing interests reported.

Periodic theta and spectral–memory relationships differentiate amnestic mild cognitive impairment from healthy aging

Camille Bouhour[1], Vincent Rochas[2,3], Mohamed Eshmawey[4], Paul G. Unschuld[3,4], Lucie Bréchet[1*]

[1*] Department of Clinical Neurosciences, University of Geneva, Geneva, 1211, Switzerland.

[2] M/EEG & Neuromod Platform, neuro @campusbiotech, Geneva, 1202, Switzerland.

[3] Department of Psychiatry, University of Geneva, Geneva, 1201, Switzerland.

[4] Geriatric Psychiatry Service, University Hospitals of Geneva (HUG), Thônex, 1226, Switzerland.

*Corresponding author: Lucie Bréchet, PhD**.** E- mail: lucie.brechet@unige.ch
Contributing authors: Camille.bouhour@unige.ch; vincent.rochas@fcbg.ch; mohamed.eshmawey@hug.ch; paul.unschuld@hug.ch.

Abstract

BACKGROUND

Amnestic mild cognitive impairment (aMCI) carries an elevated risk of progression to Alzheimer's disease, yet no reliable resting-state electroencephalography (EEG) signature has separated it from healthy aging. Disease-related information may lie in spectral power itself, in how spectral activity relates to cognition, or in both. Standard analyses also conflate oscillatory changes with aperiodic background activity.

METHODS

In this cross-sectional study, we combined sensor- and individualized source-level analyses with spectral parameterization of high-density resting-state EEG from 150 participants (34

aMCI patients, 58 healthy older adults, 58 healthy younger adults) and tested how oscillatory activity related to memory within memory-network regions.

RESULTS

Both older groups showed higher beta and gamma power and flatter aperiodic slopes relative to younger adults, consistent with known aging effects. The clearest distinction between aMCI and healthy aging was in periodic theta. Patients showed higher theta than healthy older adults and resembled younger adults, an effect standard spectral analyses missed. Source-level gamma and beta power was associated with worse memory in aMCI but not healthy older adults, though only the precuneus beta difference was confirmed between groups. Age was more closely associated with slope flattening in patients than in healthy older adults.

CONCLUSION

These findings suggest that aMCI is distinguished from healthy aging not by the magnitude of spectral change, which the groups largely shared, but by specific alterations in oscillatory activity and its link to cognition. Elevated periodic theta and the altered precuneus beta–memory relationship stood out most and are promising markers for longitudinal work.

Keywords: Amnestic mild cognitive impairment; resting-state EEG; source localization; theta oscillations; aperiodic slope; memory networks

1. Introduction

Mild cognitive impairment (MCI), a condition in which cognitive decline is greater than expected for age and education but does not meet the full clinical criteria for dementia, is associated with an increased risk of progression to Alzheimer's disease (AD).(1) The amnestic subtype (aMCI) is marked by predominant learning and memory decline, with an annual conversion rate to AD of approximately 10–15% in clinical samples.(2) aMCI is etiologically heterogeneous, however, and not all cases reflect underlying AD pathology. Because

neurodegeneration is well established by the time cognitive symptoms appear, accurately characterizing aMCI is critical for identifying at-risk individuals while decline is still limited.

Electroencephalography (EEG) provides a non-invasive and inexpensive measure of neural dynamics that may be disrupted early in the disease process.(3) Resting-state EEG power spectrum analysis quantifies oscillatory activity across frequency bands and has been used extensively to characterize aging and cognitive decline.(4,5) In healthy aging, delta and theta power progressively decreases while beta power increases, alongside slowing of the posterior alpha rhythm, reflected in a reduction in individual alpha peak frequency (IAPF).(6–8) AD shows the opposite pattern, with increased delta and theta activity and reduced alpha and beta power, reflecting progressive disruption of cortical networks.(4,9) In MCI, findings are less consistent, varying across frequency bands.(4) Theta is particularly informative, moving in opposite directions in the two groups, decreasing in healthy aging but increasing in AD. Whether it retains the age-related reduction in aMCI or diverges toward the AD-like pattern remains unclear.

Part of this inconsistency may be methodological. Standard spectral analysis conflates oscillatory activity with the aperiodic background of the EEG signal, a 1/f-like slope often described as “neural noise” that changes with age independently of oscillations.(10) This aperiodic component is thought to reflect the excitation/inhibition (E/I) balance of neural circuits, i.e., the relative contributions of excitatory and inhibitory synaptic activity, and flattens with age in a way that can mask genuine oscillatory differences.(11,12) Parameterization methods such as Fitting Oscillations and One-Over-f (FOOOF) address this by separating periodic and aperiodic components.(11,13) Fixed canonical bands carry a related risk: A shift of the individual alpha peak toward slower frequencies can present as increased theta power, and differences in band boundaries, source reconstruction and region selection may contribute

to the heterogeneity across the AD continuum.(14) In healthy aging, a steeper slope is associated with better cognitive performance, suggesting the aperiodic component is functionally meaningful rather than mere noise.(15,16) Whether this slope-cognition link holds in aMCI is not known.

The link between spectral power and cognition is also underexplored in memory-specific neural circuits. In healthy adults, resting-state gamma shows mixed relationships with memory performance: positive associations over frontal and temporal electrodes and negative associations over posterior and central sites.(17) Sex differences have also been reported in beta- and gamma-band coherence, with higher values in males.(18,19) At the preclinical stage, the relationship between oscillatory activity and pathological burden may be non-linear: Elevated high-frequency power appears at intermediate amyloid β (Aβ) load and has been interpreted as a compensatory response that eventually fails.(20) Whether elevated beta and gamma in memory networks in aMCI reflect a similar transitional state, and whether their relationship to memory performance differs from healthy aging, remains unknown.

Individualized source localization using participant-specific magnetic resonance imaging (MRI) improves anatomical specificity over group-averaged approaches,(21) but its combination with spectral parameterization remains underexplored in aMCI, particularly regarding memory performance, age and sex. The present study addresses these gaps using high-density resting-state EEG recorded from patients with aMCI, healthy older adults and healthy younger adults. We combined sensor- and individualized source-level analyses with FOOOF spectral parameterization and memory-network region-of-interest (ROI) regression to determine whether aMCI differs from healthy aging in spectral activity itself, in the relationship between oscillatory activity and memory performance or in both. We hypothesized that aMCI would show band-specific spectral alterations and altered activity-cognition relationships

relative to healthy aging. Predictions were non-directional, and comparisons across frequency bands were treated as exploratory.

2. Methods

Full methodological details are provided in the *Supplementary Methods*.

2.1. Participants and recruitment

The sample comprised 150 participants across three groups: 34 patients with aMCI (13 female; 71.59 ± 6.73 years), 58 healthy older adults (33 female; 71.31 ± 8.04 years) and 58 healthy younger adults (32 female; 25.83 ± 4.16 years). All participants gave written informed consent, and the study was approved by the Cantonal Ethical Committee of Geneva in accordance with the Declaration of Helsinki (2013).

This sample is drawn from two previous studies of the same cohort.(22,23) One hundred and forty six participants overlap with ref 22 and 148 with ref 23. Recruitment, inclusion and exclusion criteria and the full neuropsychological battery for the aMCI cohort are also described there. Patients were recruited from the Memory Center of Geneva University Hospitals. Biomarker data, including Aβ, tau, and FDG-PET, ApoE ε4 genotype, visual MRI ratings and probable etiology, were available for a subset of patients and are described in the *Supplementary Methods*.

Two measures derived from the neuropsychological battery are central to the present analyses. The Montreal Cognitive Assessment (MoCA) is a global cognitive screen scored out of 30, with scores below 26 indicating impairment.(24) The Memory Index Score (MIS), derived from the MoCA's delayed recall items, captures both free and cued recall and ranges from 0 to 15, making it more sensitive to memory-specific decline than the total MoCA.(25)

2.2. Procedure

Each participant completed a single session at Campus Biotech (Geneva, Switzerland) between March 2023 and September 2025, identical across groups. The session included the neuropsychological assessment, a 10-minute MRI acquisition of T1- and T2-weighted images and a five-minute eyes-closed resting-state EEG. These formed part of a larger protocol with additional cognitive paradigms not reported here.

2.3. MRI acquisition

Structural MRI data were acquired at Campus Biotech using a 3T Siemens MAGNETOM Prisma scanner with a 64-channel head coil. High-resolution T1-weighted images were obtained using a magnetization-prepared rapid acquisition gradient echo (MPRAGE) sequence (*TR* = 2300 ms, *TE* = 2.25 ms, *TI* = 900 ms, *voxel size* = 1 × 1 × 1 mm, *flip angle* = 8°).

2.4. EEG recording and preprocessing

Participants sat in a dark, sound-attenuated, electrically shielded room and were asked to relax with their eyes closed for five minutes. Resting EEG was acquired from a 256-channel HydroCel Geodesic sensor net connected to an EGI GES 400 amplifier. Impedance was kept as low as possible (<30 kΩ) before recording the signal at a sampling rate of 1000 Hz.

Unless otherwise stated, preprocessing was performed in Cartool 5.06.04.(26) Recordings were downsampled to 250 Hz and reduced to 204 channels by removing cheek and nape electrodes. A 1–70 Hz band-pass was applied with an eighth-order Butterworth filter, and a notch filter at 50 Hz to suppress line noise. All processing was carried out on continuous data.

The recordings were then visually inspected and marked for bad channels and bad time segments. The remaining EEGs were decomposed using independent component analysis (ICA) after excluding previously identified bad channels. The ICA decomposition was computed in MATLAB R2022a using the runica (Infomax) algorithm via FieldTrip's ft_componentanalysis function. Components reflecting artifacts such as eye movements, eye

blinks, heartbeat and muscle tension were identified by their topography and time course and removed from the reconstructed signal.

The signal from the channels previously identified as bad was then interpolated from neighbouring electrodes using Cartool's 3D spherical spline method. EEG signals were re-referenced from the hardware Cz reference to the average reference. A spatial filter was applied in Cartool to smooth the scalp topographies.(27)

2.5. EEG analyses

2.5.1. Sensor- and source-level

Sensor-level power spectral density (PSD), which describes how signal power is distributed across frequencies, was computed in Python (MNE 1.10.1)(28) on non-overlapping five-second epochs using Welch's method (1–70 Hz; 2 sec segments, mean-detrended, no overlap), after rejecting bad epochs. We averaged across segments and epochs, then normalized by the average broadband PSD. This homogenizes power magnitudes across participants, since absolute magnitudes are influenced by anatomical factors such as skull thickness and brain-to-sensor distance.

Source PSD was estimated from individualized LORETA head models built in Cartool from each participant's T1 MPRAGE, and normalized as for the sensor data.(29) The full source pipeline, including the head-model construction, solution grid and inverse projection, is detailed in the Supplementary Methods.

2.5.2. Region of interest parcellation

Source points were parcellated using the Automated Anatomical Labelling atlas version 1 (AAL)(30) on an MNI template. Twenty-two a priori memory network ROIs were selected for the regression analyses: Bilateral hippocampus, parahippocampal gyrus, anterior and posterior

cingulate, precuneus, angular gyrus and occipito-temporal regions (middle and inferior occipital gyri, lingual gyrus, calcarine cortex, inferior temporal gyrus).

2.5.3. Aperiodic and periodic spectral parameterization

The absolute PSD, averaged across the whole scalp and not broadband-normalized as in the sensor- and source-level analyses, was modelled into periodic and aperiodic components using the FOOOF toolbox 1.1.1 in Python.(11) The periodic spectrum was divided into low-frequency (1–8 Hz), alpha (8–12 Hz), beta (12–30 Hz) and gamma (30–60 Hz) bands. Band-pass filtering at 1–70 Hz produced a roll-off in power approaching the upper cut-off. Because the aperiodic component is fitted across the entire range,(11) we restricted the model fit to 1–60 Hz. The periodic gamma band is therefore narrower than the 30–70 Hz gamma used in the sensor-, source- and ROI-level analyses. Further details are given in the *Supplementary Methods*.

2.6. Statistical analyses

Analyses were performed in Python (SciPy, statsmodels 0.14.5). Unless stated otherwise, all tests were two-tailed at $\alpha = 0.05$, with Benjamini-Hochberg False Discovery Rate (FDR) correction applied for multiple comparisons. Age and sex were included as covariates in all regression models, given their established effects on EEG spectral and aperiodic measures. Cohen's d was computed for all pairwise comparisons as group A minus group B in the order reported (aMCI vs HO, aMCI vs HY, HO vs HY), so negative values indicate lower values in the first group. Because several comparisons were nonparametric, Cohen’s d is reported as a descriptive standardized mean difference rather than a test-derived effect size. We did not perform an a priori power analysis, and randomization was not applicable given the observational cross-sectional design. Sample sizes were determined by feasibility and are comparable to prior resting-state EEG studies in aMCI.(4,20) For the aMCI versus healthy

older adult comparisons, the smallest standardized difference detectable with 80% power at α = 0.05 (two-tailed) was d = 0.64 in the FOOOF subsample and d = 0.61 in the full sample, so smaller effects, including the null group interactions, could not be detected reliably. All analyses used the full sample (aMCI n = 34, HO n = 58, HY n = 58) except the FOOOF-based analyses, which used the subset passing quality control (aMCI n = 30, HO n = 57, HY n = 58). Analyses used complete cases, with no imputation of missing values. Participants were excluded from a given analysis if they lacked the relevant data: those failing FOOOF quality control ($R^2 < 0.80$) for the aperiodic analyses, and those without a detectable peak for alpha peak frequency. Group comparisons of demographic and cognitive characteristics for both samples are detailed in the *Supplementary Methods*.

Sensor- and source-level group comparisons used cluster-based permutation tests (CBPT). Adjacency was defined over space, following the electrode or source distribution, and over neighbouring frequency bins. Groups were compared pairwise using one-way F-tests with 1000 permutations and threshold-free cluster enhancement (TFCE: h = 2.0, e = 0.5),(31) and clusters were considered significant at $p < 0.01$. For each significant cluster we reported the minimum p-value, maximum F-value and mean Cohen's d with 95% confidence interval per frequency band. Bins between 48.5 and 51.5 Hz were excluded from band-level summaries because of notch attenuation, leaving 135 analysable bins across 1–70 Hz.

Source power was averaged within each of the 22 a priori ROIs, using the frequency bands that showed significant group differences in the CBPT analyses. These were beta and gamma in aMCI, and low-frequency, beta and gamma in healthy older adults. Power was regressed on MIS or MoCA with age and sex as covariates. Models were fitted with ordinary least squares (OLS) and robust standard errors (HC3) to account for potential heteroscedasticity. Predictors and outcomes were z-standardized before fitting, so coefficients are comparable across regions

and bands. We reported bootstrap confidence intervals and considered associations significant at FDR-corrected $p < 0.05$.

To test whether these memory-power associations differed between aMCI patients and healthy older adults, we pooled the two groups ($n = 92$) and fitted group × MIS, group × age and group × sex interactions in a single model. Power was extracted from the same aMCI-defined clusters in both groups, and testing was restricted to the ROI and band combinations showing significant MIS associations in aMCI. Because predictors and outcomes were standardized across the pooled sample, these coefficients are not directly comparable to the within-group estimates. Interaction terms and model assumption diagnostics are reported in the Supplementary Methods.

FOOOF aperiodic parameters (offset, exponent) and periodic band power were compared across groups using Kruskal-Wallis omnibus tests, FDR-corrected within the aperiodic and periodic families separately. Significant omnibus effects were followed by pairwise Mann-Whitney U tests, FDR-corrected across the three group comparisons. Alpha peak frequency was compared using the same approach.

To relate aperiodic activity to cognition, we regressed the aperiodic exponent on cognitive score (z-standardized MIS or MoCA) with age and sex as covariates, separately within each group. To test whether the exponent-cognition association differed between groups, we pooled aMCI patients and healthy older adults ($n = 87$) and fitted group × score, group × age and group × sex interactions in a single model, with each interaction family FDR-corrected independently.

3. Results

From the parent cohort of 60 healthy older adults, 60 younger adults and 34 aMCI patients,(22,23) four were excluded for missing data: three (two older, one younger) lacked an MRI scan and one younger adult lacked MoCA and MIS scores. The analysed sample

comprised 34 aMCI patients, 58 healthy older adults and 58 younger adults, with age and sex available for all. FOOOF-based analyses used the subset passing quality control (30, 57 and 58, respectively), and alpha peak frequency the subset with a detectable peak (29, 55 and 56, respectively).

3.1. Demographic and cognitive group comparisons

Age differed significantly across groups ($F(2,74.89) = 1139.07$, $p < 0.001$), with healthy younger adults (HY; $n = 58$, 32 females, 25.83 ± 4.16 years) substantially younger than both healthy older adults (HO; $n = 58$, 33 females, 71.31 ± 8.04 years; $t(85.50) = 38.28$, $p < 0.001$, $d = 7.11$) and aMCI patients (aMCI; $n = 34$, 13 females, 71.59 ± 6.73 years; $t(48.03) = 35.82$, $p < 0.001$, $d = 8.71$; *Supplementary Table 1*). No difference in age emerged between aMCI and healthy older adults ($t(79.16) = -0.18$, $p = 0.859$, $d = 0.04$), confirming group matching.

MIS differed significantly across groups ($H(2) = 28.99$, $p < 0.001$), with aMCI patients showing lower performance (8.82 ± 4.14) relative to healthy older (12.74 ± 3.08; $d = -1.12$, $p < 0.001$) and healthy younger adults (13.29 ± 2.76; $d = -1.34$, $p < 0.001$), validating diagnostic classification. MoCA similarly differed ($H(2) = 42.77$, $p < 0.001$), with lower values in aMCI (23.32 ± 4.02) versus healthy older adults (26.72 ± 2.60; $d = -1.06$, $p < 0.001$) and healthy younger adults (28.09 ± 1.74; $d = -1.70$, $p < 0.001$). Healthy younger and healthy older adults differed significantly on MoCA despite both falling within cognitively normal ranges ($d = -0.62$, $p = 0.003$). The three groups were sex matched ($\chi^2(2) = 3.37$, $p = 0.185$).

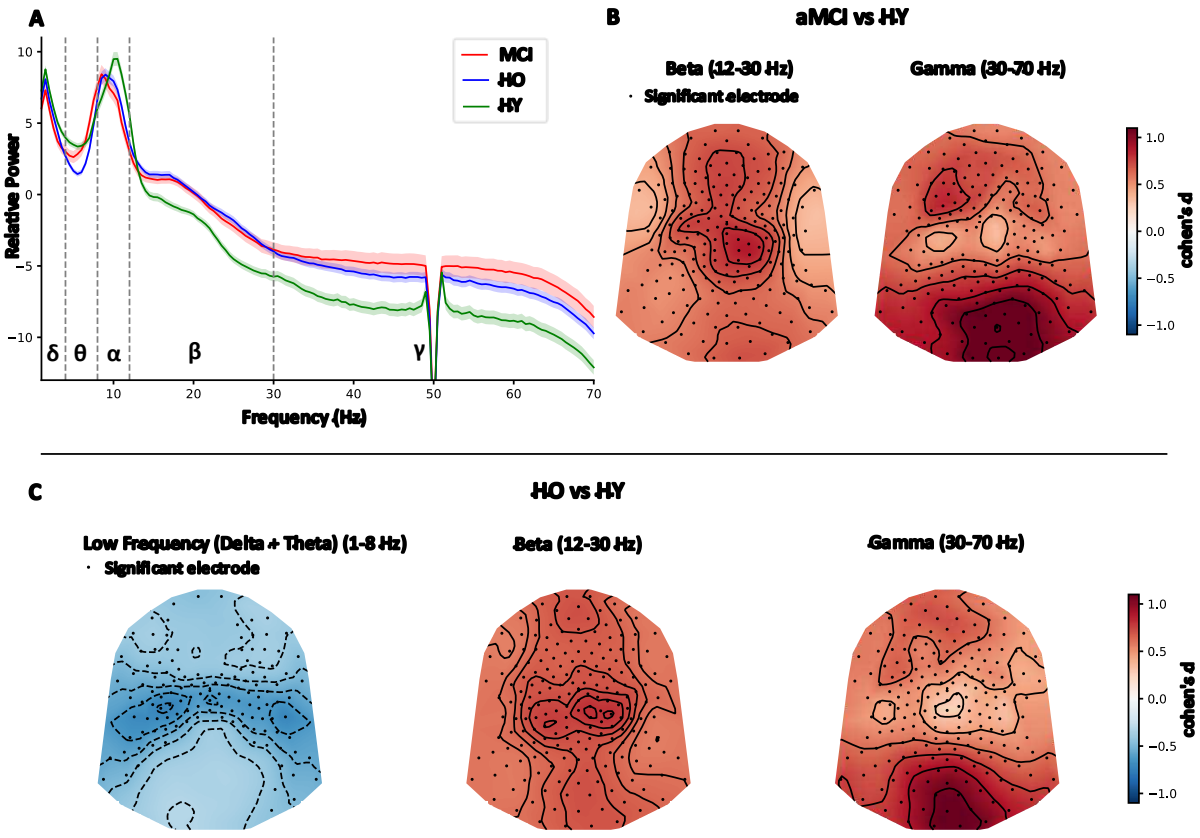
Demographic and cognitive group comparisons in the retained FOOOF subsample (aMCI: $n = 30$, 13 females, 71.27 ± 6.84 years, $R^2 = 0.98 \pm 0.02$; HO: $n = 57$, 32 females, 71.02 ± 7.79 years, $R^2 = 0.98 \pm 0.02$; HY: $n = 58$, 32 females, 25.83 ± 4.16 years, $R^2 = 0.99 \pm 0.02$) reproduced those of the full sample, with aMCI and healthy older adults remaining matched on

age and sex and aMCI patients remaining impaired on both MIS and MoCA relative to the two control groups; no comparison changed in significance (*Supplementary Table 2*).

3.2. Sensor-level power spectral density analyses

Group-averaged sensor-level PSDs showed expected resting-state characteristics, including prominent alpha peaks across all groups (**Fig. 1A**). Descriptively, younger adults showed higher low-frequency and alpha power but lower beta and gamma power than both older groups, whose profiles were broadly similar.

Figure 1 Sensor-level power spectral density and cluster-based permutation topographies reveal significant group differences in frequency distributions.



(**A**) Group-averaged power spectral density across 1–70 Hz for patients with amnestic mild cognitive impairment (aMCI; n = 34), healthy older adults (HO; n = 58) and healthy younger adults (HY; n = 58), normalized to broadband power and averaged over the whole scalp. Vertical dotted lines delineate the frequency bands as delta, 1–4 Hz (δ), theta, 4–8 Hz (θ), alpha, 8–12 Hz (α), beta, 12–30 Hz (β) and gamma, 30–70 Hz (γ). (**B** and **C**) Topographic maps displaying significant sensor-level Cohen's d effect sizes from cluster-based permutation tests (CBPT; 1,000 permutations, threshold-free cluster enhancement (TFCE), $p < 0.01$) comparing

aMCI vs. HY (**B**) and HO vs. HY (**C**). Black marker dots indicate electrodes with significant differences. The colour scale represents the mean Cohen's d within frequency bands, with warmer red colours indicating larger positive effect sizes and cooler blue colours indicating larger negative effect sizes.

CBPT revealed widespread significant clusters between aMCI and healthy younger adults, spanning nearly all 204 electrodes and 109 of 135 frequency bins. aMCI patients showed increased power relative to younger adults, moderate in beta (13–30 Hz; $d = 0.56$, $p \leq 0.001$) over central electrodes and larger in gamma (30–70 Hz; $d = 0.79$, $p \leq 0.001$) over posterior electrodes (**Fig. 1B**). Healthy older adults also differed widely from younger adults (204 electrodes, 114 frequency bins), showing the same beta and gamma increases, alongside a theta reduction (4–6 Hz; $d = -0.53$, $p = 0.002$) not seen in aMCI (**Fig. 1C**). No clusters distinguished aMCI from healthy older adults (all $p > 0.01$; **Table 1**).

Table 1 Sensor-level group CBPT comparisons of power spectral density across frequency bands

Group Comparison	Electrodes, Freq Bins	F-stat	Cohen's d	95% CI	p-value
Low frequency (1–8 Hz)					
aMCI vs HO	—	66.35	0.19	[−0.30, 0.65]	0.247
aMCI vs HY	—	84.69	−0.29	[−0.75, 0.15]	0.144
HO vs HY	129/204, 5/15	244.22	−0.53	[−0.91, −0.17]	0.002 **
Alpha (8–12 Hz)					
aMCI vs HO	—	34.88	−0.17	[−0.65, 0.27]	0.639
aMCI vs HY	—	78.97	−0.52	[−1.00, −0.10]	0.167
HO vs HY	—	81.72	−0.41	[−0.80, −0.04]	0.136
Beta (12–30 Hz)					
aMCI vs HO	—	43.95	−0.21	[−0.62, 0.22]	0.493
aMCI vs HY	202/204, 35/37	427.80	0.56	[0.14, 1.08]	≤0.001 ***
HO vs HY	204/204, 35/37	493.85	0.75	[0.40, 1.16]	≤0.001 ***
Gamma (30–70 Hz)					
aMCI vs HO	—	54.18	0.26	[−0.23, 0.71]	0.346
aMCI vs HY	184/204, 74/74	428.09	0.79	[0.37, 1.23]	≤0.001 ***
HO vs HY	203/204, 74/74	482.43	0.75	[0.39, 1.18]	≤0.001 ***

aMCI $n = 34$, HO $n = 58$, HY $n = 58$. Statistics computed using cluster-based permutation tests (CBPT) with 1,000 permutations and threshold-free cluster enhancement (TFCE). Electrodes, Freq Bins = number of significant electrodes from CBPT out of 204 and the number of significant frequency bins out of those available in each band (135 in total across 1–70 Hz, excluding notch bins between 48.5–51.5 Hz);

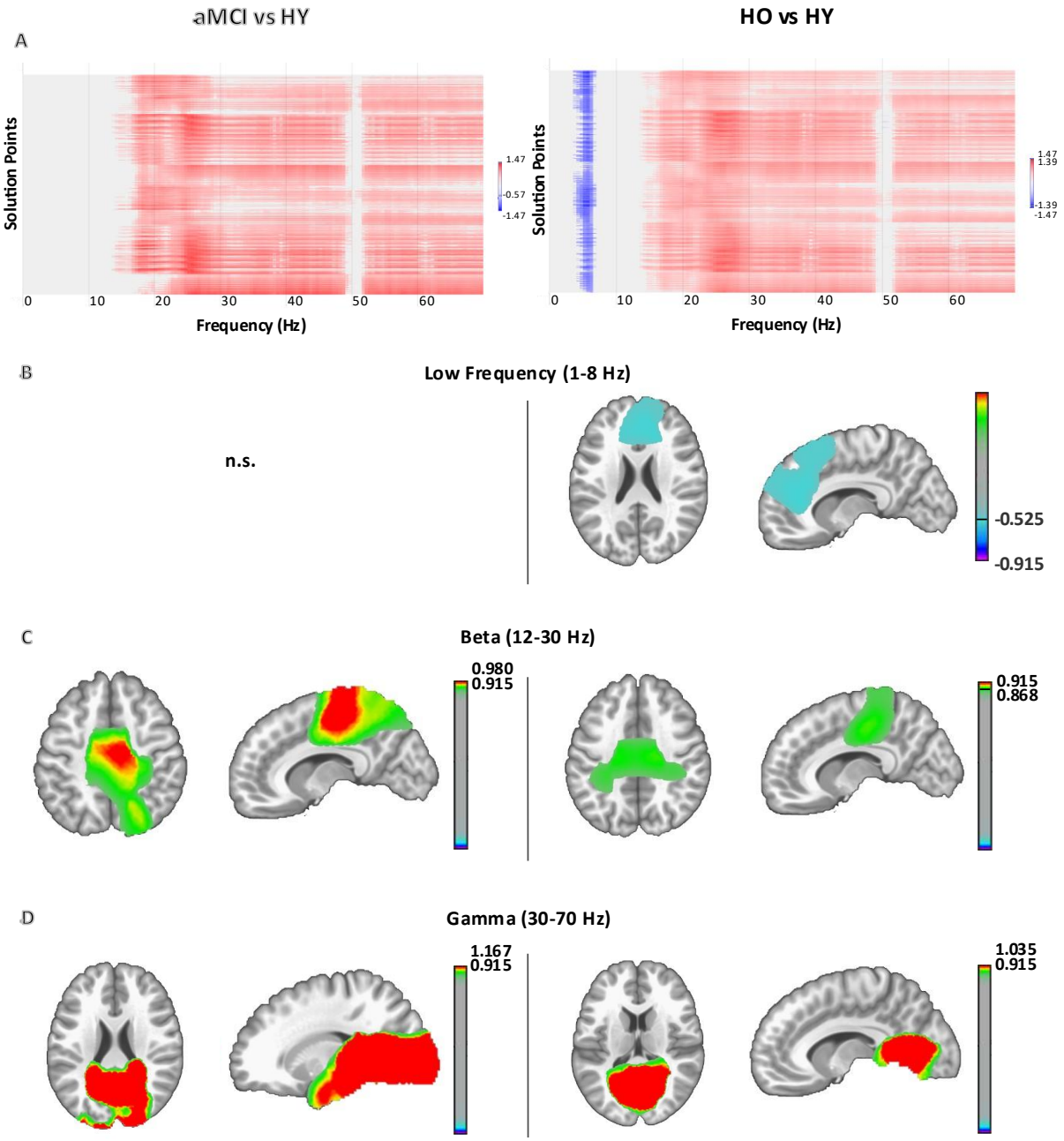
F-stat = maximum F-statistic within band; Cohen's d = standardized mean difference estimated across all electrodes and frequency bins within each band; 95% CI = 95% confidence interval; p-value = minimum p-value within band ($p \leq 0.001$ is the lowest attainable value with 1,000 permutations); — = non-significant comparisons ($p \geq 0.01$). ** $p < 0.01$; *** $p \leq 0.001$.

3.3. Source-level power spectral density analyses

Individualized source-level PSD analyses converged with the sensor-level findings, with significant clustering patterns confined to specific frequency ranges (**Fig. 2A**, *Supplementary Table 3*).

In aMCI versus younger adults, significant effects spanned beta (13.5–30 Hz) and gamma (30–69.5 Hz). In healthy older versus younger adults, significant effects also included a low-frequency reduction within 3–6.5 Hz. This continuous, unidirectional pattern spanned both the delta and theta ranges, so we refer to this as a combined low-frequency band (1–8 Hz) for interpretation. Across significant clusters, source-level CBPT results revealed near whole-brain effects, involving all 5,845 solution points in the beta band and 5,607 to 5,820 of 5,845 in the gamma band (*Supplementary Table 3*). In aMCI versus younger adults, increased beta power in aMCI patients ($d = 0.63$, $p \leq 0.001$) had the most pronounced effect sizes in medial frontal, precentral, paracentral, postcentral and cingulate regions **(Fig. 2C)**, while increased gamma power ($d = 0.89$, $p \leq 0.001$) was strongest in occipital regions (lingual gyrus, cuneus) and the posterior cingulate cortex **(Fig. 2D)**. In healthy older versus younger adults, the low-frequency pattern showed reduced power in older adults ($d = -0.63$, $p \leq 0.001$) in frontal (medial and superior frontal gyri) and limbic regions (anterior cingulate cortex (ACC), cingulate gyrus) **(Fig. 2B)**. Beta-band increases ($d = 0.76$, $p \leq 0.001$) were most prominent in medial frontal, precentral, paracentral, cingulate, postcentral and inferior parietal regions **(Fig. 2C)**, while gamma-band increases ($d = 0.86$, $p \leq 0.001$) were strongest in posterior cingulate, occipital (cuneus, lingual gyrus, precuneus) and parietal regions **(Fig. 2D)**. No clusters separated aMCI from healthy older adults.

Figure 2 Source-level distributions of CBPT effect sizes show significant group differences in PSD.



(**A**) Cohen's d effect sizes for differences identified by cluster-based permutation tests (CBPT), shown across solution points and frequencies (1,000 permutations, threshold-free cluster enhancement (TFCE), $p < 0.01$) for the two main group comparisons (amnestic mild cognitive impairment (aMCI) $n = 34$ vs. healthy younger (HY) $n = 58$ and healthy older (HO) $n = 58$ vs. HY $n = 58$), illustrating which frequencies contained significant differences based on LORETA inverse solutions of power spectral density (PSD). Grey indicates solution points and frequencies without significant differences, and the gap at 48.5–51.5 Hz corresponds to bins excluded because of notch-filter attenuation. A common colour scale limit of ±1.47 is applied across both comparisons. (**B**, **C** and **D**) Spatial distribution of source-level Cohen's d effect

sizes per frequency band (low frequency 1–8 Hz, beta 12–30 Hz and gamma 30–70 Hz, respectively) mapped onto an MRI template for anatomical reference, masked at the CBPT significance threshold ($p < 0.01$). In B–D, a common colour scale limit of ±0.915 (the mean of the maximum absolute effect sizes across all bands) is applied for visual consistency across comparisons and frequency bands; n.s. indicates comparisons without significant clusters at the specified threshold.

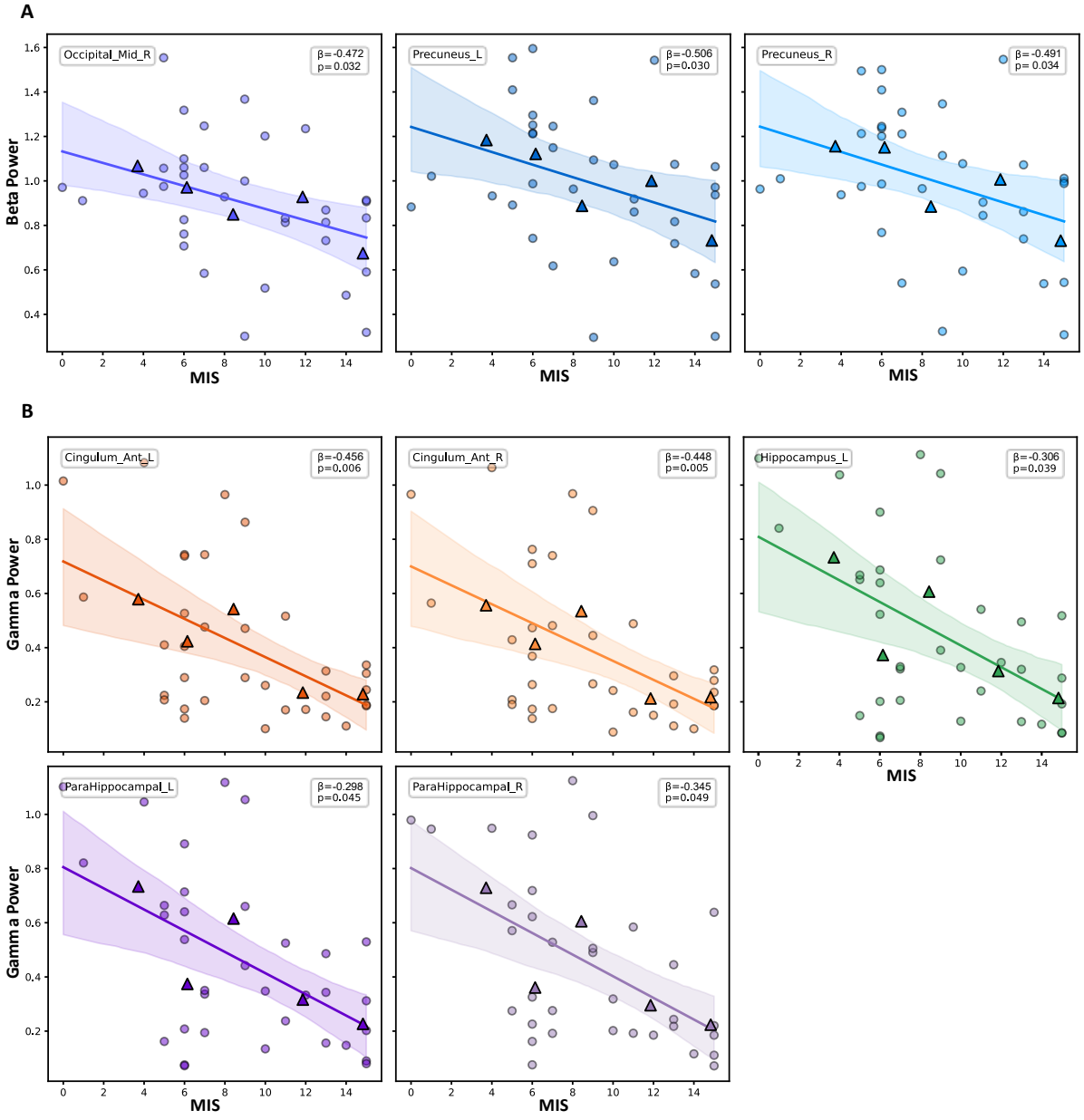
3.4. Memory network region of interest regression analyses

In aMCI patients, the MIS showed significant negative associations with beta- and gamma-band power across several regions, whereas MoCA showed no significant relationships with beta- or gamma-band power in any ROI. The right middle occipital gyrus displayed higher beta power with worse memory performance ($\beta = -0.47$, *95% CI* [−0.88, −0.20], $p = 0.032$). This relationship was also evident bilaterally in the precuneus (right: $\beta = -0.49$, *95% CI* [−0.88, −0.20], $p = 0.034$; left: $\beta = -0.51$, *95% CI* [−0.89, −0.20], $p = 0.030$; **Fig. 3A**). Gamma-band power showed parallel negative associations with MIS across the medial temporal lobe and cingulate regions. The bilateral ACC showed higher gamma power with worse memory scores (right: $\beta = -0.45$, *95% CI* [−0.70, −0.21], $p = 0.005$; left: $\beta = -0.46$, *95% CI* [−0.74, −0.18], $p = 0.006$). The left hippocampus showed a similar negative relationship ($\beta = -0.31$, *95% CI* [−0.53, −0.07], $p = 0.039$), as did the bilateral parahippocampal gyrus (right: $\beta = -0.35$, *95% CI* [−0.58, −0.03], $p = 0.049$; left: $\beta = -0.30$, *95% CI* [−0.52, −0.05], $p = 0.045$; **Fig. 3B**). Leave-one-out refits produced stable coefficients in all eight regions. Full regression results for all 22 ROIs in both groups, including age and sex effects, are reported in *Supplementary Tables 4* (aMCI) *and 5* (healthy older adults), with the covariate findings described in the Supplementary Results.

We conducted a parallel analysis in healthy older adults across the same 22 memory network ROIs and found no significant associations between cognitive scores and power in any ROI or band. We then fitted group × MIS, group × age and group × sex interactions in the eight ROI-band combinations showing significant MIS associations in aMCI (three beta, five gamma;

Fig. 3). Selection on the aMCI associations inflates these interaction estimates, which we therefore treat as exploratory.

Figure 3 MIS associations with beta- and gamma-band power in memory network ROIs in aMCI patients.



(**A and B**) Linear regression results showing significant associations between Memory Index Score (MIS) and (**A**) beta-band (12–30 Hz) and (**B**) gamma-band (30–70 Hz) power across memory network regions of interest (ROI) in amnestic mild cognitive impairment (aMCI) patients (n = 34). Each subplot displays individual data points (circles), binned means (triangles), regression lines and bootstrapped 95% confidence intervals (shaded regions). Models were fitted by ordinary least squares (OLS) with age and sex as covariates and robust

standard errors (HC3). Standardized beta estimates (β) and false discovery rate (FDR)-corrected p-values are shown for all significant associations. Negative coefficients indicate higher power associated with worse memory performance.

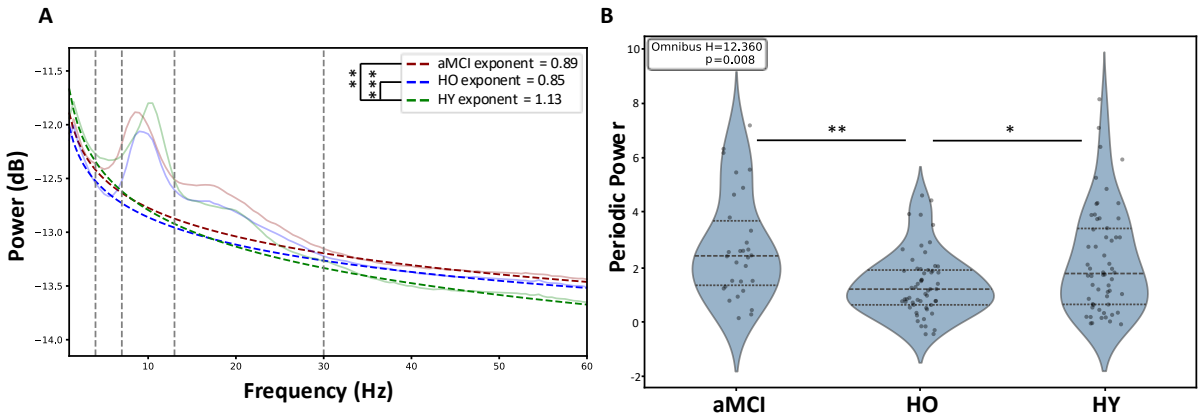
Only precuneus beta showed a significant interaction (right: $\beta = 0.63$, *95% CI* [0.24, 1.08], $p = 0.019$; left: $\beta = 0.62$, *95% CI* [0.22, 1.06], $p = 0.019$), stable under leave-one-out refitting. The right middle occipital gyrus did not survive correction ($\beta = 0.46$, $p = 0.061$). No gamma interaction was significant ($\beta = 0.08$ to 0.24, all $p \geq 0.587$), with wide confidence intervals that do not distinguish a shared association from a group difference. Group × age and group × sex interactions were not significant in any region (all FDR $p \geq 0.36$).

Age and sex covariates also showed significant relationships with gamma-band power. In aMCI patients, age was positively associated with gamma across medial-temporal, occipital, cingulate and precuneus regions, controlling for cognitive score and sex (all $p < 0.05$; *Supplementary Table 4*), with further parietal, occipital and temporal regions reaching significance for MoCA but not MIS. In healthy older adults, age showed no significant gamma associations (*Supplementary Table 5*). Males showed higher gamma power than females across overlapping medial-temporal and occipital regions in both older groups (all $p < 0.05$; *Supplementary Tables 4 and 5*). Age or sex did not predict beta power in either group or low-frequency power in healthy older adults.

3.5. Aperiodic and periodic spectral parameterization

Model quality control ($R^2 > 0.8$) excluded four aMCI patients and one healthy older adult for poor fit. Model fit in the retained sample was high across groups (mean $R^2 = 0.98$–0.99; aMCI $n = 30$, HO $n = 57$, HY $n = 58$). The aperiodic component analysis included the exponent and offset parameters **(Fig. 4A)**. All pairwise p-values reported below are FDR-corrected across the three group comparisons.

Figure 4 FOOOF analysis of spectral characteristics across groups.



(**A**) Aperiodic fits (1/f slopes) displayed on log-log plots of the channel-averaged power spectrum for each group (amnestic mild cognitive impairment (aMCI) n = 30, healthy older (HO) n = 57, healthy younger (HY) n = 58). The dashed lines represent the fitted aperiodic component for each group (aMCI = red, HO = blue, HY = green), demonstrating the characteristic 1/f scaling of the neural power spectrum. (**B**) Significant group differences in periodic theta power (low-frequency band, 1–8 Hz) across all groups, shown as violin plots with overlaid individual data points and quartile indicators. Asterisks indicate significant group pair differences (* $p < 0.05$, ** $p < 0.01$, *** $p < 0.001$, following false discovery rate (FDR) correction). All analyses employed non-parametric Kruskal-Wallis tests with pairwise Mann-Whitney U comparisons and FDR correction ($\alpha = 0.05$).

The exponent, which quantifies the steepness of the 1/f power-law decay, differed significantly across groups ($H(2) = 28.51$, $p < 0.001$). Both aMCI patients (0.89 ± 0.34; $U = 506$, $p = 0.002$; $d = -0.84$) and healthy older adults (0.85 ± 0.26; $U = 717$, $p < 0.001$; $d = -1.09$) showed flatter slopes than younger adults (1.13 ± 0.26), while aMCI patients and healthy older adults did not differ ($U = 955$, $p = 0.374$; $d = 0.14$). The offset, the intercept of the aperiodic fit and hence a measure of broadband power expressed as $\log_{10}$ power in V^2 Hz^{-1}, followed the same pattern ($H(2) = 26.71$, $p < 0.001$), with aMCI patients (-11.89 ± 0.33; $U = 596$, $p = 0.024$; $d = -0.63$) and healthy older adults (-12.02 ± 0.28; $U = 729$, $p < 0.001$; $d = -1.08$) showing more negative offsets than healthy younger adults (-11.66 ± 0.36). aMCI patients and healthy older adults did not differ significantly ($U = 1056$, $p = 0.073$; $d = 0.43$).

We quantified oscillatory activity from the power spectrum across the four predefined frequency bands. The low-frequency band (1-8 Hz) showed a significant group effect ($H(2)$ =

12.36, $p = 0.008$; **Fig. 4B),** driven by a periodic peak at 6.2–6.6 Hz, within the theta range. We therefore refer to it as periodic theta hereafter. Periodic theta power was higher in aMCI patients (2.76 ± 1.90) than in healthy older adults (1.37 ± 1.17; $U = 1253$, $p = 0.001$; $d = 0.94$). Healthy younger adults (2.24 ± 1.92) also showed higher theta power than healthy older adults ($U = 1264$, $p = 0.045$; $d = -0.55$) but did not differ from aMCI patients ($U = 1018$, $p = 0.194$; $d = 0.27$). No group effects were observed for alpha ($H(2) = 4.63$, $p = 0.197$), beta ($H(2) = 0.29$, $p = 0.867$) or gamma periodic power ($H(2) = 2.16$, $p = 0.452$). Alpha peak frequency was detected in 29 of 30 aMCI patients, 55 of 57 healthy older adults and 56 of 58 healthy younger adults and differed significantly across groups ($H(2) = 23.79$, $p < 0.001$). Healthy younger adults showed higher alpha peak frequencies (10.42 ± 0.78 Hz) than both aMCI patients (9.44 ± 0.89 Hz; $U = 345$, $p < 0.001$; $d = -1.18$) and healthy older adults (9.65 ± 1.02 Hz; $U = 885$, $p < 0.001$; $d = -0.84$), who did not differ ($U = 699$, $p = 0.357$; $d = -0.22$).

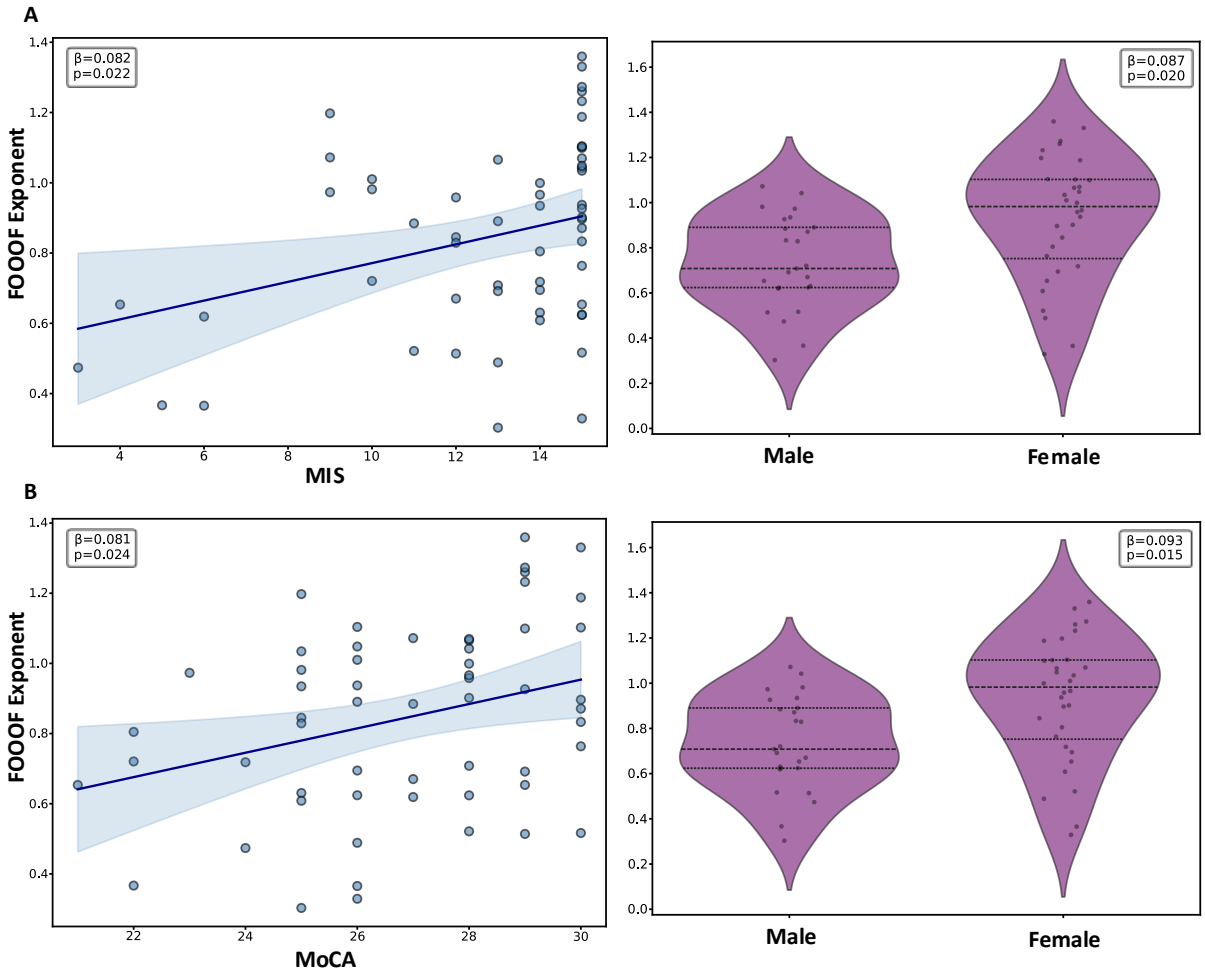
3.6. Associations between aperiodic activity and cognition

In aMCI ($n = 30$), cognitive scores did not significantly predict the exponent (MIS model: $F(3, 26) = 5.74$, $p = 0.004$, *adjusted* $R^2 = 0.33$; MIS: $\beta = 0.31$, *95% CI* [−0.02, 0.64], $p = 0.097$; MoCA model: $F(3, 26) = 3.99$, $p = 0.018$, *adjusted* $R^2 = 0.24$; MoCA: $\beta = 0.05$, *95% CI* [−0.29, 0.39], $p = 0.761$). Age was a significant negative predictor in both models (MIS: $\beta = -0.44$, *95% CI* [−0.79, −0.10], $p = 0.038$; MoCA: $\beta = -0.54$, *95% CI* [−0.89, −0.19], $p = 0.022$), indicating flatter aperiodic slopes with increasing age (*Supplementary Fig. 1*).

In healthy older adults ($n = 57$), higher cognitive performance was significantly associated with steeper slopes in both models (MIS model: $F(3, 53) = 5.88$, $p = 0.002$, *adjusted* $R^2 = 0.21$; MIS: $\beta = 0.31$, *95% CI* [0.07, 0.56], $p = 0.027$; MoCA model: $F(3, 53) = 5.69$, $p = 0.002$, *adjusted* $R^2 = 0.20$; MoCA: $\beta = 0.31$, *95% CI* [0.06, 0.56], $p = 0.027$; **Fig. 5A and B**, left). Sex was also a significant predictor, with females showing larger exponents than males (MIS: $\beta = 0.33$, *95%*

CI [0.08, 0.58], $p = 0.027$; MoCA: $\beta = 0.36$, *95% CI* [0.11, 0.60], $p = 0.027$; **Fig. 5A and B**, right). Age was not a significant predictor (MIS: $\beta = -0.15$, *95% CI* [−0.40, 0.09], $p = 0.260$; MoCA: $\beta = -0.04$, *95% CI* [−0.30, 0.21], $p = 0.735$).

Figure 5 Associations between aperiodic exponent, cognitive performance and sex in healthy older adults.



Significant multiple linear regression effects are shown, with the Fitting Oscillations and One-Over-f (FOOOF) aperiodic exponent as the outcome, estimated using ordinary least squares (OLS). Left panels show cognitive associations: (**A**) Memory Index Score (MIS) and (**B**) Montreal Cognitive Assessment (MoCA), each adjusted for age and sex. Blue points represent individual participants, the dark blue line the fitted regression slope and the shaded area the 95% confidence interval. The right panels show sex effects from models that include age and either (**A**) MIS or (**B**) MoCA as covariates. Violin plots display the distribution of the exponent by sex with individual data points overlaid. Standardized beta estimates (β) and false discovery rate (FDR)-corrected p-values are shown for all significant associations. Healthy older adults: $n = 57$ (male $n = 25$, female $n = 32$). Only significant effects are displayed.

Pooling both groups (n = 87) with group × score, group × age and group × sex interaction terms, neither score interaction was significant (group × MIS: $\beta = -0.02$, *95% CI* [−0.49, 0.39], $p = 0.921$; group × MoCA: $\beta = 0.36$, *95% CI* [−0.09, 0.79], $p = 0.248$), so the slope-cognition association did not differ significantly between groups. Group × sex was also non-significant (both $p = 0.923$). The group × age interaction was significant in the MoCA model ($\beta = 0.65$, *95% CI* [0.18, 1.05], $p = 0.009$) and not significant in the MIS model ($\beta = 0.44$, *95% CI* [−0.07, 0.84], $p = 0.050$). The significant estimate was positive, indicating that age was more strongly tied to slope flattening in aMCI than in healthy older adults.

4. Discussion

This study examined whether aMCI differs from healthy aging in spectral activity itself, in how that activity relates to cognition, or in both. Aging and aMCI shared broad spectral features, but aMCI was distinguished by specific alterations in oscillatory activity and its relationship to cognition rather than by the magnitude of spectral change.

4.1. Spectral changes are shared by aging and aMCI, but theta reduction is specific to healthy aging

Widespread beta and gamma increases in both older groups, with no difference between them, are consistent with reported effects of aging in these bands.(5–7)

The frontocentral and cingulate beta increases have an established interpretation. Age-related sensorimotor beta increases have been linked to reduced inhibitory efficiency,(6,9,32) and comparable frontocentral increases to the recruitment of additional processing resources.(5) The parallel beta increases in both older groups suggest an age-related rather than disease-specific mechanism.

Gamma increases showed a posterior distribution. Eyes-closed recording in a shielded room, sensor-source convergence and overlap with visual and default mode regions are consistent with a neural contribution, but high-frequency EEG remains vulnerable to residual myogenic contamination,(33) and the strong sex effect in temporal gamma makes this an alternative explanation that cannot be excluded. Gamma oscillations depend on fast-spiking GABAergic interneurons,(9) and the posterior cingulate and neighbouring occipital regions are key episodic and visual working memory nodes,(9,34) included among the a priori ROIs used in the cognition regression analyses.

The theta reduction in healthy older adults, absent in aMCI, replicates a well-established aging pattern.(4,8) The failure of aMCI patients to show this reduction may indicate that they retain a profile more similar to younger adults. Alternatively, the relative preservation of theta could reflect early pathological changes, consistent with documented theta increases seen in AD.(4,6) AD was the most likely etiology in only a minority of our patients, so this reading applies to a subset.

Reduced IAPF in both older groups, without a further reduction in aMCI, suggests slowing that follows the aging trajectory rather than additional disease-specific change.(4) Elevated theta in a fixed band can also reflect a downward shift of the alpha peak rather than a genuine low-frequency change.(14) This is unlikely here, since IAPF did not differ between aMCI and healthy older adults and periodic peaks were fitted per participant.

4.2. Associations between memory network oscillations and cognitive impairment

In aMCI, worse memory tracked higher beta and gamma power across memory network regions, but only the precuneus beta association was confirmed to differ between groups. The apparent specificity of the gamma associations should therefore be read with caution. MoCA

showed no associations in either group, consistent with its role as a global screen.(24) The precuneus is a core node of the default mode network, with established roles in episodic memory retrieval and self-referential processing.(34) Beta oscillations are thought to maintain the current cognitive state, holding information online rather than updating it.(32,35) Elevated resting beta may therefore reflect memory circuits held in a maintenance state and less available for flexible encoding and retrieval. In healthy older adults, higher resting beta has been interpreted as a favourable sign of preserved function,(5) whereas our finding of higher beta with worse memory in aMCI suggests that this relationship differs in the disease context.

In both high-frequency bands, higher power tracked worse memory in aMCI. This may mark a transitional state in which high-frequency upregulation has exceeded the range that supports cognition. This is consistent with a proposed non-linear trajectory in which early high-frequency increases reflect compensation that is eventually overwhelmed as pathology progresses.(20) The medial-temporal regions carrying the gamma association are among the earliest affected in aMCI and AD,(36) and gamma there depends on parvalbumin-positive GABAergic interneurons that are disrupted in AD.(37,38) These mechanisms are inferred from work on AD and were not established in the present, etiologically heterogeneous cohort.

These findings fit a broader picture of default mode dysregulation in aMCI. Reports of beta change in MCI are mixed in direction,(39) and our regional, source-level finding may help explain some of this variability. The present results also converge with independent structural evidence from an overlapping sample of the same cohort. Hippocampal volume is reduced in aMCI relative to both control groups and, within patients, predicts delayed verbal recall.(23) Together, these measures support the view of aMCI as a memory network-level disorder across both structure and function.

4.3. Aperiodic slope and its relationship to cognition

Both older groups showed flatter aperiodic slopes than younger adults, consistent with the neural noise hypothesis of aging.(10,12) In healthy older adults, steeper slopes were associated with better cognitive performance, replicating recent findings,(15,16) and females showed steeper slopes than males. Although this slope-cognition association was not evident in aMCI, the two groups did not differ, so we cannot conclude that the relationship itself is disrupted in aMCI rather than simply harder to detect in a smaller sample.

In aMCI, the aperiodic slope was more strongly tied to age than to cognition, and this age relationship was stronger in patients than in healthy older adults, supported by the group × age interaction in the MoCA model. This is consistent with a shift toward supercritical dynamics and increased functional E/I in MCI,(40) changes associated with longitudinal progression.(15,40) Aperiodic and E/I measures have been reported to differ across stages of the AD continuum, with the clearest disruption at the dementia stage.(41) Thus, the clearest alteration in aperiodic dynamics in aMCI was not a demonstrated loss of the slope-cognition relationship, but a stronger link between age and slope flattening.

4.4. Elevated periodic theta in aMCI as altered age-related theta dynamics

Elevated periodic theta was the clearest spectral difference distinguishing aMCI from healthy older adults and emerged only once periodic and aperiodic components were separated. aMCI patients resembled younger adults more than their age-matched peers. Unlike the memory associations, which were largely shared between the older groups, this one directly distinguished aMCI from healthy aging.

Periodic beta/theta ratios have been shown to differentiate MCI from controls where full-spectrum measures do not, precisely because the aperiodic component masks oscillatory differences.(13) Theta plays a central role in hippocampal-dependent memory processes,(42)

so elevated periodic theta in aMCI may reflect altered hippocampal function, although the present difference was measured at the whole-scalp level and was not localized. In AD, theta power and inter-regional coherence both increase, opposite to the decline seen in healthy aging, a pattern thought to mark neurodegeneration rather than preserved function.(4,6,43) Higher theta power need not mean that theta still coordinates the high-frequency activity involved in memory encoding, a form of cross-frequency coupling reported as altered in aging and AD.(10,43) Whether this elevated theta reflects preserved function or early pathology remains open, a distinction that will require longitudinal or biomarker-linked data to resolve.

4.5. Limitations and future directions

Sample sizes were modest, particularly for the aperiodic analyses after FOOOF quality control (aMCI $n = 30$) and the ROI regressions (aMCI $n = 34$). Although AD was the most prevalent etiology and a subset of patients had supportive Aβ, tau or FDG-PET findings, biomarkers were not obtained systematically. LORETA assumes a degree of spatial smoothness, which limits precise anatomical localization. Education was unavailable for both control groups and could not be modelled as a covariate. Non-significant aMCI versus healthy older adult comparisons carry non-trivial effect sizes at this sample size and should not be read as evidence of equivalence. These findings derive from a single-site sample: patients recruited through clinical referral and healthy participants through community outreach. Generalisation to other settings, to biomarker-confirmed cohorts, or to community-dwelling MCI not seeking clinical assessment therefore requires confirmation.

Future work should examine cross-frequency coupling, particularly theta-gamma phase-amplitude coupling in hippocampal-prefrontal circuits, to test whether theta-gamma coordination is altered during memory processing in aMCI.(10,43) The signatures identified here, elevated periodic theta, the precuneus beta–memory relationship and the medial-temporal

gamma associations, are promising candidates for longitudinal tracking of AD conversion, and confirming which replicate will require larger samples. Longitudinal magnetoencephalography (MEG) work in adults at familial risk shows that spectral power adds prognostic value for progression to MCI beyond Aβ and tau biomarkers.(14) Whether those MEG effects generalize to more accessible EEG measures is an important direction for translation.

5. Conclusion

Both older groups showed spectral changes, flatter slopes and elevated beta and gamma, consistent with age-related changes in excitation-inhibition-related dynamics. What set aMCI apart was more specific than any global shift. Periodic theta did not show the reduction seen in healthy aging, the one spectral feature that distinguished patients from healthy older adults directly. The relationship between precuneus beta and memory also differed between groups, the only memory association confirmed to do so. Age, rather than cognition, was more strongly tied to aperiodic slope flattening in patients than in controls. Together, these findings place the distinction between aMCI and healthy aging not in the magnitude of spectral change, which the groups largely shared, but in specific alterations of spectral activity and its link to memory. Periodic theta and precuneus beta offer the clearest evidence and the most promising targets for longitudinal and interventional work.

Supplementary information. The following article contains supplementary methods, tables, and a figure.

List of Abbreviations.

- **AAL:** Automated Anatomical Labeling
- **ACC:** anterior cingulate cortex
- **AD:** Alzheimer's disease

- **aMCI:** amnestic mild cognitive impairment
- **Aβ:** amyloid-beta
- **CBPT:** cluster-based permutation test
- **CI:** confidence interval
- **E/I:** excitation/inhibition
- **EEG:** electroencephalography
- **FDG-PET:** fluorodeoxyglucose positron emission tomography
- **FDR:** false discovery rate
- **FOOOF:** Fitting Oscillations and One-Over-f
- **GABA:** gamma-aminobutyric acid
- **HC3:** heteroscedasticity-consistent standard errors (type 3)
- **HO:** healthy older adults
- **HY:** healthy younger adults
- **IAPF:** individual alpha peak frequency
- **ICA:** independent component analysis
- **LORETA:** low-resolution brain electromagnetic tomography
- **MCI:** mild cognitive impairment
- **MEG:** magnetoencephalography
- **MIS:** Memory Index Score
- **MNI:** Montreal Neurological Institute

- **MoCA:** Montreal Cognitive Assessment
- **MPRAGE:** magnetization-prepared rapid acquisition gradient echo
- **MRI:** magnetic resonance imaging
- **OLS:** ordinary least squares
- **PSD:** power spectral density
- **ROI:** region of interest
- **TFCE:** threshold-free cluster enhancement

Declarations

Ethics approval and consent to participate

The study was approved by the Cantonal Ethical Committee of Geneva in accordance with the Declaration of Helsinki (2013) with number CCER 2021-01388 and is registered on clinicaltrials.gov: https://clinicaltrials.gov/study/NCT05710549. All participants could provide informed consent and gave their written informed consent prior to participation in the study.

Consent for publication

Not applicable.

Availability of data and materials

Patient anonymized data supporting the findings of this study are available from the corresponding author upon reasonable request.

Competing interests

The authors report no competing interests.

Funding

This work was supported by the Dementia Research Switzerland – Synapsis Foundation (grant number 2024-CAD03) and the Swiss National Science Foundation (grant number PZ00P1_208686).

Authors' contributions

L.B., C.B., and V.R. designed the research; L.B. and C.B. collected the data; C.B. and V.R. analyzed the data; C.B., L.B., and V.R. wrote the paper; M.E. and P.G.U. edited and revised the manuscript; L.B. supervised the research and secured funding.

Acknowledgements

We thank the Dementia Research Switzerland – Synapsis Foundation (grant number 2024-CAD03) and the Swiss National Science Foundation (grant number PZ00P1_208686) for funding this work. This work was supported by the M/EEG & Neuromod platform at neuro@campusbiotech, Geneva, Switzerland. We thank the Memory Center of Geneva University Hospitals for participant recruitment and the Memstim laboratory members for data collection throughout the study.

References

1. Stokin GB, Krell-Roesch J, Petersen RC, Geda YE. Mild Neurocognitive Disorder: An Old Wine in a New Bottle. Harv Rev Psychiatry. 2015 Sep;23(5):368–76. doi:10.1097/HRP.0000000000000084

2. Anderson ND. State of the science on mild cognitive impairment (MCI). CNS Spectr. 2019 Feb;24(1):78–87. doi:10.1017/S1092852918001347

3. Olejniczak P. Neurophysiologic Basis of EEG: J Clin Neurophysiol. 2006 Jun;23(3):186–9. doi:10.1097/01.wnp.0000220079.61973.6c

4. Meghdadi AH, Stevanović Karić M, McConnell M, Rupp G, Richard C, Hamilton J, et al. Resting state EEG biomarkers of cognitive decline associated with Alzheimer's disease and mild cognitive impairment. Ginsberg SD, editor. PLOS ONE. 2021 Feb 5;16(2):e0244180. doi:10.1371/journal.pone.0244180

5. Barry RJ, De Blasio FM. EEG differences between eyes-closed and eyes-open resting remain in healthy ageing. Biol Psychol. 2017 Oct;129:293–304. doi:10.1016/j.biopsycho.2017.09.010

6. Aoki Y, Hata M, Iwase M, Ishii R, Pascual-Marqui RD, Yanagisawa T, et al. Cortical electrical activity changes in healthy aging using EEG-eLORETA analysis. Neuroimage Rep. 2022 Dec;2(4):100143. doi:10.1016/j.ynirp.2022.100143

7. Perinelli A, Assecondi S, Tagliabue CF, Mazza V. Power shift and connectivity changes in healthy aging during resting-state EEG. NeuroImage. 2022 Aug;256:119247. doi:10.1016/j.neuroimage.2022.119247

8. Cummins TDR, Finnigan S. Theta power is reduced in healthy cognitive aging. Int J Psychophysiol. 2007 Oct;66(1):10–7. doi:10.1016/j.ijpsycho.2007.05.008

9. Jafari Z, Kolb BE, Mohajerani MH. Neural oscillations and brain stimulation in Alzheimer's disease. Prog Neurobiol. 2020 Nov;194:101878. doi:10.1016/j.pneurobio.2020.101878

10. Voytek B, Kramer MA, Case J, Lepage KQ, Tempesta ZR, Knight RT, et al. Age-Related Changes in 1/ *f* Neural Electrophysiological Noise. J Neurosci. 2015 Sep 23;35(38):13257–65. doi:10.1523/JNEUROSCI.2332-14.2015

11. Donoghue T, Haller M, Peterson EJ, Varma P, Sebastian P, Gao R, et al. Parameterizing neural power spectra into periodic and aperiodic components. Nat Neurosci. 2020 Dec;23(12):1655–65. doi:10.1038/s41593-020-00744-x

12. Gao R, Peterson EJ, Voytek B. Inferring synaptic excitation/inhibition balance from field potentials. NeuroImage. 2017 Sep;158:70–8. doi:10.1016/j.neuroimage.2017.06.078

13. Azami H, Zrenner C, Brooks H, Zomorrodi R, Blumberger DM, Fischer CE, et al. Beta to theta power ratio in EEG periodic components as a potential biomarker in mild cognitive impairment and Alzheimer's dementia. Alzheimers Res Ther. 2023 Aug 7;15(1):133. doi:10.1186/s13195-023-01280-z

14. Gallego-Rudolf J, Wiesman AI, Yakoub Y, Zetterberg H, Blennow K, Baillet S, et al. Prediction of mild cognitive impairment progression using time-sensitive multimodal biomarkers. Sci Adv. 2026 Aug 14;12(33):eaee2305. doi:10.1126/sciadv.aee2305

15. Warren TS, Shende SA, Ashrafi J, Clements GM, Mudar RA. Resting-State EEG Power and Aperiodic Activity in Individuals with Mild Cognitive Impairment and Cognitively Healthy Controls. Brain Sci. 2025 Dec 3;15(12):1305. doi:10.3390/brainsci15121305

16. Lago S, Zago S, Montemurro S, Calabrò RS, Maggio MG, Dattola S, et al. Education shapes the link between EEG aperiodic components and cognitive aging. Zhan W, editor. PLOS One. 2026 Mar 9;21(3):e0328318. doi:10.1371/journal.pone.0328318

17. Manippa V, Scaramuzzi GF, Scianatico G, Cornacchia E, Spina AC, Taurisano P, et al. Resting-state EEG gamma power predicts immediate and delayed recall in healthy adults. Cogn Neurodyn. 2025 Dec;19(1):138. doi:10.1007/s11571-025-10313-2

18. Jaušovec N, Jaušovec K. Resting brain activity: Differences between genders. Neuropsychologia. 2010 Nov;48(13):3918–25. doi:10.1016/j.neuropsychologia.2010.09.020

19. Hoshi H, Shigihara Y. Age- and gender-specific characteristics of the resting-state brain activity: a magnetoencephalography study. Aging. 2020 Nov 4;12(21):21613–37. doi:10.18632/aging.103956

20. Gaubert S, Raimondo F, Houot M, Corsi MC, Naccache L, Diego Sitt J, et al. EEG evidence of compensatory mechanisms in preclinical Alzheimer's disease. Brain. 2019 Jul 1;142(7):2096–112. doi:10.1093/brain/awz150

21. Xie W, Richards JE. Cortical Source Localization in EEG Frequency Analysis. In: Gable PA, Miller MW, Bernat EM, editors. The Oxford Handbook of EEG Frequency [Internet]. 1st ed. Oxford University Press; 2022 [cited 2026 Mar 12]. p. 377–400. Available from: https://academic.oup.com/edited-volume/44425/chapter/374614289 doi:10.1093/oxfordhb/9780192898340.013.16

22. Tarailis P, Lory K, Unschuld PG, Michel CM, Bréchet L. Self-related thought alterations associated with intrinsic brain dysfunction in mild cognitive impairment. Sci Rep. 2025 Apr 10;15(1):12279. doi:10.1038/s41598-025-97240-8

23. Bréchet L, Toussas K, Marie D, Unschuld PG. The Hippocampus Links Episodic Memory and Bodily Awareness. Brain Behav. 2026 Jul;16(7):e71570. doi:10.1002/brb3.71570

24. Nasreddine ZS, Phillips NA, Bédirian V, Charbonneau S, Whitehead V, Collin I, et al. The Montreal Cognitive Assessment, MoCA: A Brief Screening Tool For Mild Cognitive Impairment. J Am Geriatr Soc. 2005 Apr;53(4):695–9. doi:10.1111/j.1532-5415.2005.53221.x

25. Julayanont P, Brousseau M, Chertkow H, Phillips N, Nasreddine ZS. Montreal Cognitive Assessment Memory Index Score (MoCA-MIS) as a Predictor of Conversion from Mild Cognitive Impairment to A lzheimer's Disease. J Am Geriatr Soc. 2014 Apr;62(4):679–84. doi:10.1111/jgs.12742

26. Brunet D, Murray MM, Michel CM. Spatiotemporal Analysis of Multichannel EEG: CARTOOL. Comput Intell Neurosci. 2011;2011:1–15. doi:10.1155/2011/813870

27. Michel CM, Brunet D. EEG Source Imaging: A Practical Review of the Analysis Steps. Front Neurol. 2019 Apr 4;10:325. doi:10.3389/fneur.2019.00325

28. Gramfort A. MEG and EEG data analysis with MNE-Python. Front Neurosci. 2013;7. doi:10.3389/fnins.2013.00267

29. Pascual-Marqui RD, Michel CM, Lehmann D. Low resolution electromagnetic tomography: a new method for localizing electrical activity in the brain. Int J Psychophysiol. 1994 Oct;18(1):49–65. doi:10.1016/0167-8760(84)90014-X

30. Tzourio-Mazoyer N, Landeau B, Papathanassiou D, Crivello F, Etard O, Delcroix N, et al. Automated Anatomical Labeling of Activations in SPM Using a Macroscopic Anatomical Parcellation of the MNI MRI Single-Subject Brain. NeuroImage. 2002 Jan;15(1):273–89. doi:10.1006/nimg.2001.0978

31. Smith S, Nichols T. Threshold-free cluster enhancement: Addressing problems of smoothing, threshold dependence and localisation in cluster inference. NeuroImage. 2009 Jan 1;44(1):83–98. doi:10.1016/j.neuroimage.2008.03.061

32. Engel AK, Fries P. Beta-band oscillations — signalling the status quo? Curr Opin Neurobiol. 2010 Apr;20(2):156–65. doi:10.1016/j.conb.2010.02.015

33. Muthukumaraswamy SD. High-frequency brain activity and muscle artifacts in MEG/EEG: a review and recommendations. Front Hum Neurosci. 2013;7. doi:10.3389/fnhum.2013.00138

34. Buckner RL, Andrews-Hanna JR, Schacter DL. *The Brain's Default Network*: *Anatomy, Function, and Relevance to Disease*. Ann N Y Acad Sci. 2008 Mar;1124(1):1–38. doi:10.1196/annals.1440.011

35. Wang XJ. Neurophysiological and Computational Principles of Cortical Rhythms in Cognition. Physiol Rev. 2010 Jul;90(3):1195–268. doi:10.1152/physrev.00035.2008

36. Braak H, Braak E. Neuropathological stageing of Alzheimer-related changes. Acta Neuropathol (Berl). 1991 Sep;82(4):239–59. doi:10.1007/BF00308809

37. Bartos M, Vida I, Jonas P. Synaptic mechanisms of synchronized gamma oscillations in inhibitory interneuron networks. Nat Rev Neurosci. 2007 Jan;8(1):45–56. doi:10.1038/nrn2044

38. Bi D, Wen L, Wu Z, Shen Y. GABAergic dysfunction in excitatory and inhibitory (E/I) imbalance drives the pathogenesis of Alzheimer's disease. Alzheimers Dement. 2020 Sep;16(9):1312–29. doi:10.1002/alz.12088

39. Zawiślak-Fornagiel K, Ledwoń D, Bugdol M, Grażyńska A, Ślot M, Tabaka-Pradela J, et al. Quantitative EEG Spectral and Connectivity Analysis for Cognitive Decline in Amnestic Mild Cognitive Impairment. J Alzheimers Dis. 2024 Jan 30;97(3):1235–47. doi:10.3233/JAD-230485

40. Javed E, Suárez-Méndez I, Susi G, Román JV, Palva JM, Maestú F, et al. A Shift Toward Supercritical Brain Dynamics Predicts Alzheimer's Disease Progression. J Neurosci. 2025 Feb 26;45(9):e0688242024. doi:10.1523/JNEUROSCI.0688-24.2024

41. Van Nifterick AM, Mulder D, Duineveld DJ, Diachenko M, Scheltens P, Stam CJ, et al. Resting-state oscillations reveal disturbed excitation–inhibition ratio in Alzheimer's disease patients. Sci Rep. 2023 May 7;13(1):7419. doi:10.1038/s41598-023-33973-8

42. Herweg NA, Solomon EA, Kahana MJ. Theta Oscillations in Human Memory. Trends Cogn Sci. 2020 Mar;24(3):208–27. doi:10.1016/j.tics.2019.12.006

43. Chen X, Li Y, Li R, Yuan X, Liu M, Zhang W, et al. Multiple cross-frequency coupling analysis of resting-state EEG in patients with mild cognitive impairment and Alzheimer's disease. Front Aging Neurosci. 2023 Aug 4;15:1142085. doi:10.3389/fnagi.2023.1142085

Supplementary Files

This is a list of supplementary files associated with this preprint. Click to download.

- BouhourSupplementaryADresearchtherapy.pdf
- BouhourSupplementaryTables45.xlsx